

# The synthesis and characterisation of some closed polyhedral metallocarbon clusters<sup>1</sup>

John E. Davies<sup>a</sup>, Brian F.G. Johnson<sup>a,\*</sup>, Caroline M. Martin<sup>a</sup>, Ruth H.H. Pearson<sup>a</sup>,  
Paul J. Dyson<sup>b</sup>

<sup>a</sup> Department of Chemistry, University of Cambridge, Lensfield Road, Cambridge, CB2 1EW, UK

<sup>b</sup> Department of Chemistry, Imperial College of Science, Technology and Medicine, South Kensington, London, SW7 2AY, UK

Received 12 May 1997

---

## Abstract

Ligands containing unsaturated C<sub>2</sub> and C<sub>4</sub> units have been reacted with triruthenium dodecacarbonyl to produce new organometallic clusters with simple *closo*-Ru<sub>x</sub>C<sub>y</sub> polyhedral frameworks which may be regarded as *quasi*-carboranes. The thermolysis of [Ru<sub>3</sub>(CO)<sub>12</sub>] with 1,4-diphenylbutadiene yields the new clusters [Ru<sub>3</sub>(CO)<sub>8</sub>(μ<sub>3</sub>-CPh(CH)<sub>2</sub>CPh)] **2** and [Ru<sub>4</sub>(CO)<sub>9</sub>(μ<sub>4</sub>-CPhCCH<sub>2</sub>CH<sub>2</sub>Ph)] **3**, while treatment of a solution of [Ru<sub>3</sub>(CO)<sub>12</sub>] and diphenylacetylene with trimethylamine N-oxide (Me<sub>3</sub>NO) yields [Ru<sub>2</sub>(CO)<sub>6</sub>(μ-{C<sub>2</sub>Ph<sub>2</sub>}<sub>2</sub>CO)] **4** as the major product and the new cluster [Ru<sub>4</sub>(CO)<sub>11</sub>(μ<sub>4</sub>-C<sub>2</sub>Ph<sub>2</sub>)<sub>2</sub>] **5**. The solid-state structures of **2**, **3** and **5** have been established by single crystal X-ray diffraction analyses and are shown to possess *closo*-Ru<sub>3</sub>C<sub>4</sub> pentagonal bipyramidal, *closo*-Ru<sub>4</sub>C<sub>2</sub> octahedral and *closo*-Ru<sub>4</sub>C<sub>4</sub> dodecahedral skeletons, respectively. The structure and bonding in all three clusters may be rationalised using the Wade–Mingos polyhedral skeletal electron pair approach. © 1998 Elsevier Science S.A.

**Keywords:** Triruthenium dodecacarbonyl; Organometallic clusters; *closo*-Ru<sub>x</sub>C<sub>y</sub> polyhedral frameworks

---

## 1. Introduction

Organometallic cluster chemistry continues to grow rapidly and an ever increasing array of complicated structures containing metallo- and carbo-units is emerging. In general, these compounds are regarded as basic metallic cluster units onto which an organic moiety is grafted. This has its uses and, for example, has assisted greatly in our understanding of the nature of the interaction of species, such as alkenes, alkynes or arenes with the metallic surface [1]. Nonetheless, this view is restricted and it is more convenient, certainly from the view of predicting new organometallic species and their shape, to consider the structures of many organometallic clusters, particularly those derived from alkenes and alkynes, as the metallo equivalents of the carboranes.

In the early 1970's, Wade developed a set of electron counting rules to account for the structural complexity and bonding interactions in the borane clusters. These rules have subsequently been extended to the Polyhedral Skeletal Electron Pair Theory (PSEPT) which, together with isolobal relationships, may be used to rationalise the structures observed in many of the cluster types known today, including the mixed transition metal—main group clusters incorporating both metal and carbon atoms in their molecular skeletons [2–4]. Thus, for example, since the M(CO)<sub>3</sub> unit (M = Fe, Ru, Os) is isoelectronic and isolobal with BH, it follows that all compounds [B<sub>n</sub>H<sub>n</sub>]<sup>2-</sup> and [B<sub>n-2</sub>C<sub>2</sub>H<sub>n</sub>]<sup>2-</sup> should have equivalents such as [M<sub>n</sub>(CO)<sub>3n</sub>]<sup>2-</sup> or [M(CO)<sub>3</sub>]<sub>n-2</sub>C<sub>2</sub>R<sub>2</sub>. Such metallocarbon clusters generally conform to the borane structural pattern and Fig. 1 illustrates some of the different metallocarbon polyhedra which have been observed for metals of the iron triad. These include MC<sub>2</sub> (e.g. [Fe(CO)<sub>4</sub>(η<sup>2</sup>-CH<sub>2</sub>CH<sub>2</sub>)] [5]), M<sub>2</sub>C<sub>2</sub> (e.g. [Fe<sub>2</sub>(CO)<sub>6</sub>(μ-Me<sub>3</sub>C<sub>4</sub>Me<sub>3</sub>)] [6]), M<sub>3</sub>C (e.g. [Fe<sub>3</sub>(CO)<sub>8</sub>(η<sup>5</sup>-Cp)(μ<sub>3</sub>-CMe)] [7]), MC<sub>4</sub> (e.g. [Fe(CO)<sub>3</sub>(η<sup>4</sup>-cyclobutadiene)] [8]) and

---

\* Corresponding author.

<sup>1</sup> Dedicated to Professor Ken Wade on the occasion of his 65th birthday in recognition of his outstanding contributions to cluster chemistry.

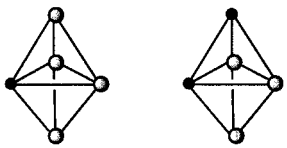
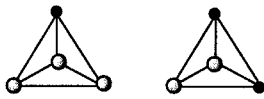

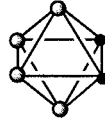

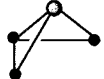
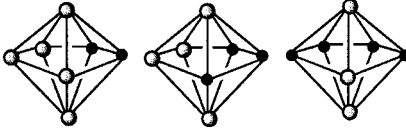

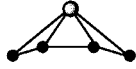
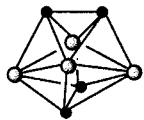
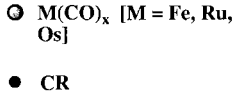
	<i>Closo-</i> (n + 1) SEPs	<i>Nido-</i> (n + 2) SEPs	<i>Arachno-</i> (n + 3) SEPs
<b>Trigonal Bipyramid</b> 6 SEPs	$M_4C$ $M_3C_2$ 	$M_3C$ $M_2C_2$ 	$MC_2$ 
<b>Octahedron</b> 7 SEPs	$M_4C_2$ 	$M_3C_2$ $MC_4$ 	$MC_3$ 
<b>Pentagonal Bipyramid</b> 8 SEPs	$M_5C_2$ $M_4C_3$ $M_3C_4$ 	$M_3C_3$ $M_2C_4$ 	$MC_4$ 
<b>Dodecahedron</b> 9 SEPs	$M_4C_4$ 		

Fig. 1. Examples of the *closo*-, *nido*- and *arachno*-metallocarbon clusters observed for the metals of the iron triad.

[Fe(CO)<sub>3</sub>(η<sup>4</sup>-butadiene)] [5], M<sub>3</sub>C<sub>2</sub> (e.g. [HFe<sub>3</sub>(CO)<sub>9</sub>(μ<sub>3</sub>-C<sub>2</sub>Ph<sub>2</sub>)] [9] and [Os<sub>3</sub>(CO)<sub>10</sub>(μ<sub>3</sub>-C<sub>2</sub>Ph<sub>2</sub>)] [10]), M<sub>4</sub>C (e.g. [Fe<sub>4</sub>(CO)<sub>12</sub>(μ<sub>4</sub>-CCOOMe)][Et<sub>4</sub>N] [11], M<sub>2</sub>C<sub>4</sub> (e.g. [Fe<sub>2</sub>(CO)<sub>6</sub>(μ-CMe(COH)<sub>2</sub>CMe)] [12], M<sub>3</sub>C<sub>3</sub> (e.g. [HOs<sub>3</sub>(CO)<sub>9</sub>(μ<sub>3</sub>-CHCHCCHO)] [13], M<sub>4</sub>C<sub>2</sub> (e.g. [Ru<sub>4</sub>(CO)<sub>12</sub>(μ<sub>4</sub>-C<sub>2</sub>Ph<sub>2</sub>)] [14], M<sub>3</sub>C<sub>4</sub> (e.g. [Ru<sub>3</sub>(CO)<sub>8</sub>(μ<sub>3</sub>-C<sub>12</sub>H<sub>18</sub>)] [15], M<sub>4</sub>C<sub>3</sub> (e.g. [Fe<sub>4</sub>(CO)<sub>11</sub>(μ<sub>3</sub>-CHCHCMe)] [16], M<sub>5</sub>C<sub>2</sub> (e.g. in [Os<sub>6</sub>(CO)<sub>16</sub>(μ<sub>4</sub>-EtCCMe)] [17], and M<sub>4</sub>C<sub>4</sub> (e.g. [Fe<sub>4</sub>(CO)<sub>11</sub>(μ<sub>4</sub>-EtCCH<sub>2</sub>)] [18]. These clusters have either *closo*-, *nido*- or *arachno*-polyhedral cores and if capped or condensed clusters polyhedra were also considered then the list would increase in length considerably, since, for example, any alkyne bridging or capping a cluster could be included [19].

In a continuation of our studies into the reactions of transition metal carbonyl clusters with unsaturated organic ligands we now report the synthesis and characterisation of some new cluster complexes containing ruthenium and carbon skeletal atoms. Their structures have been established in the solid-state by single crystal

X-ray diffraction and rationalised using the Wade–Mingos polyhedral skeletal electron pair approach.

## 2. Results and discussion

The direct reaction of [Ru<sub>3</sub>(CO)<sub>12</sub>] **1** with 1,4-diphenylbutadiene in refluxing octane (125°C) for 5 h yields several products which may be purified by column chromatography on silica gel using hexane/dichloromethane (1:4, v/v) as the eluent. Two of these products have been characterised by spectroscopy as [Ru<sub>3</sub>(CO)<sub>8</sub>(μ<sub>3</sub>-CPh(CH)<sub>2</sub>CPh)] **2** and [Ru<sub>4</sub>(CO)<sub>9</sub>(μ<sub>4</sub>-CPhCCH<sub>2</sub>CH<sub>2</sub>Ph)] **3** and their structures confirmed by X-ray diffraction analyses (*vide infra*). Spectroscopic data for these compounds are listed in Table 1.

The mass spectrum of complex **2** contains a strong molecular ion peak at 732 (calc. = 732) amu and subsequent peaks corresponding to the consecutive loss of eight CO ligands. The <sup>1</sup>H NMR spectrum of **2** shows two multiplet resonances at δ 7.04 and 6.50 ppm with

Table 1  
Spectroscopic data for compounds 2–5

Cluster	IR ( $\nu_{\text{co}}$ $\text{cm}^{-1}$ , $\text{CH}_2\text{Cl}_2$ )	Mass spectrum ( $m/z$ )	$^1\text{H}$ NMR (ppm, $\text{CDCl}_3$ )
2	2070(m), 2031(vs), 2009(m), 1979(m), 1877(w), 1850(w).	732 (calc. 732)	3.43 (br s, 2H), 7.08–7.01 (m, 6H), 6.54–6.44 (m, 4H).
3	2063(s), 2021(s sh), 2010(vs), 1991(sh w), 1955(w sh, br).	864 (calc. 863)	7.40–7.05 (m, 5H), 6.43 (m, 1H), 5.92, (m, 1H), 5.82 (m, 1H), 5.63 (m, 1H), 5.01 (m, 1H), 4.00 (m, 1H), 3.44 (m, 1H), 2.56 (m, 1H), 2.30 (m, 1H).
4	2090(m), 2069(vs), 2028(s), 1672(m).	756 (calc. 755)	7.26 (m, 10H), 7.14 (m, 10H).
5	2084(w), 2070(vw sh), 2054(w), 2041(vs), 2025(s), 1982(m), 1942(m), 1836(w br).	1071 (calc. 1069)	6.93 (m, 12H) 6.72 (m, 8H).

relative intensities of 6:4 which may be attributed to the *meta*-/*para*- and *ortho*-protons of the two equivalent phenyl rings, respectively. A broad singlet resonance is also observed at  $\delta$  3.43 ppm with a relative intensity of 2. This latter signal indicates the presence of two equivalent olefinic protons, and hence suggests that C–H bond cleavage has occurred twice upon coordination of the diphenylbutadiene ligand to the cluster core. The

formulation of compound 2 as  $[\text{Ru}_3(\text{CO})_8(\mu_3\text{-CPh}(\text{CH})_2\text{CPh})]$  has been confirmed by a single crystal X-ray structure determination on a crystal grown from toluene at  $-25^\circ\text{C}$ .

The molecular structure of compound 2 is shown in Fig. 2 and the principal bond distances and angles are given in Table 2. Complex 2 crystallises with half a molecule in the asymmetric unit [there is a diad through

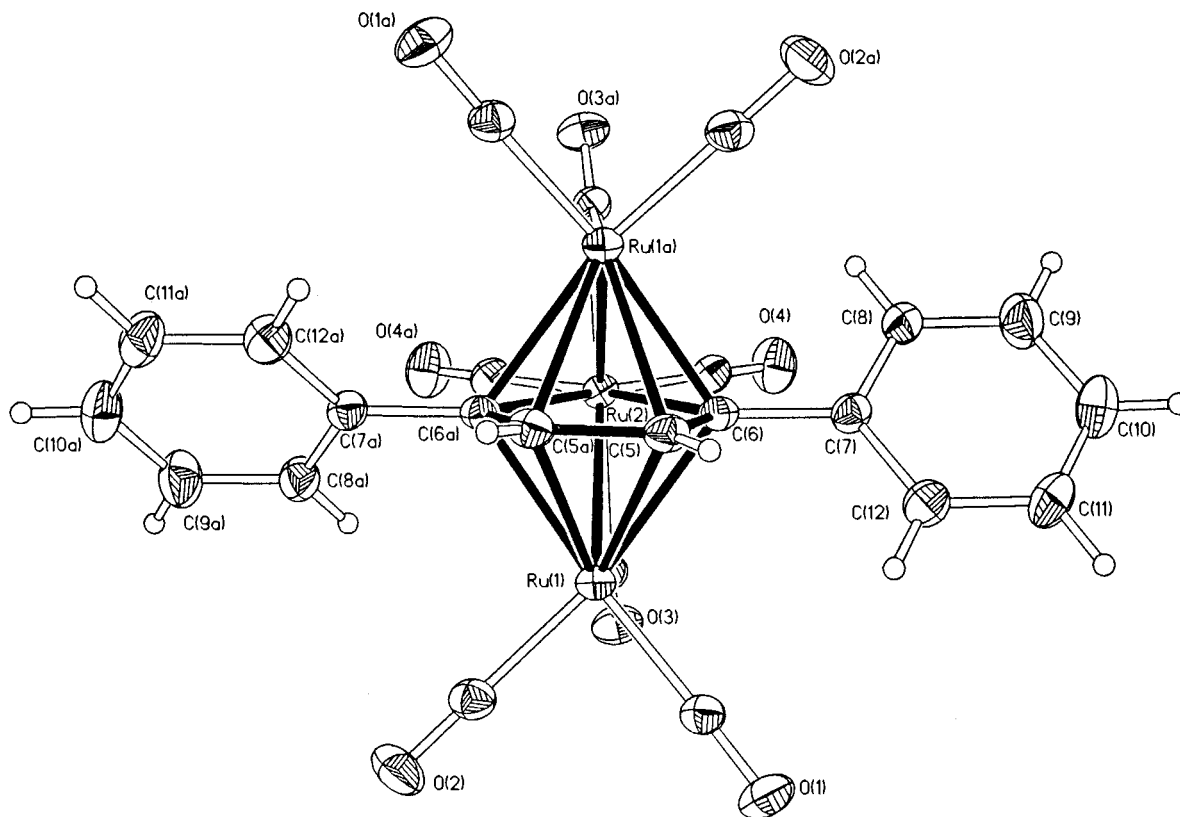


Fig. 2. Molecular structure of 2, showing the atomic labelling scheme; the C atoms of the CO groups bear the same numbering as the corresponding O atoms.

Table 2  
Bond lengths (Å) and angles (°) for **2**

Ru(1)–Ru(2)	2.6830(6)	C(5)–C(5a)	1.453(7)
Ru(1a)–Ru(2)	2.6830(6)	C(5)–C(6)	1.442(5)
Ru(1)–C(5)	2.320(4)	C(6)–C(7)	1.503(5)
Ru(1)–C(5a)	2.330(3)	Ru(1)–C(3)	2.014(4)
Ru(1)–C(6)	2.329(4)	Ru(2)–C(3)	2.170(4)
Ru(1)–C(6a)	2.287(3)	C(3)–O(3)	1.164(4)
Ru(2)–C(6)	2.208(3)	mean Ru–C <sub>(term CO)</sub>	1.896(4)
Ru(2)–C(6a)	2.208(3)	mean C–O <sub>(term CO)</sub>	1.136(5)
		mean C–C <sub>(phenyl)</sub>	1.382(7)
Ru(1)–Ru(2)–Ru(1a)	88.99(2)	C(6)–C(5)–C(5a)	114.7(2)
C(6)–Ru(2)–C(6a)	74.1(2)	Ru(2)–C(6)–C(5)	118.2(2)

Ru(2)]. The three ruthenium atoms in complex **2** adopt an open, bent arrangement with the two Ru–Ru edges [Ru(1)/Ru(1/a)–Ru(2) 2.6830(6) Å] forming an angle of 88.99(2)°. The diphenylbutadiene moiety has clearly undergone a double C–H bond activation with the elimination of H<sub>2</sub> and the ligand forms two rather long  $\sigma$ -bonds between the outer carbon atoms of the C<sub>4</sub> chain and the central ruthenium atom [Ru(2)–C(6/6a) 2.208(3) Å] giving a metallacyclopentadiene ring which is essentially planar [the largest deviation from the mean plane being 0.0158 Å at C(5)]. In addition, the *ipso*-carbons of the phenyl groups are also coplanar with the heterocycle, their displacements from the plane being only 0.018 Å, whereas the phenyl rings are orientated at an angle of 49.1° with respect to the RuC<sub>4</sub> plane. The organic moiety also interacts with the two terminal ruthenium atoms in a  $\pi$ -fashion through all four carbon atoms of the C<sub>4</sub> chain [Ru(1/a)–C(5) 2.320(4), Ru(1/a)–C(5a) 2.330(3), Ru(1/a)–C(6) 2.329(4), Ru(1/a)–C(6a) 2.287(3) Å], and similarities in carbon–carbon bond distances [C(5)–C(6)/C(5a)–C(6a) 1.442(5), C(5)–C(5a) 1.453(7) Å] about the ruthenacyclopentadiene ring indicate the delocalised  $\pi$ -nature of the system. Each ruthenium atom in **2** also carries two terminal carbonyl ligands, while the remaining two CO groups asymmetrically bridge the two ruthenium–ruthenium edges [Ru(1)–C(3) 2.014(4), Ru(2)–C(3) 2.170(4) Å] of the cluster. The overall structure is very similar to that previously reported for [Ru<sub>3</sub>(CO)<sub>8</sub>(CMeC<sup>i</sup>PrCMeC<sup>i</sup>Pr)] [15] and [Fe<sub>3</sub>(CO)<sub>8</sub>(C<sub>4</sub>R<sub>4</sub>)] [20–23].

The M<sub>3</sub>C<sub>4</sub> skeleton in **2** may therefore be described as a *closo*-pentagonal bipyramid (one ruthenium and four carbon atoms forming the pentagonal plane and two ruthenium atoms forming the apices) which obeys the polyhedral skeletal electron pair model, i.e. 7 skeletal atoms held together by 8 (*n* + 1) skeletal electron pairs.

The infrared spectrum of **3** is very similar in terms of both profile and wavenumber to that of the known cluster, [Ru<sub>4</sub>(CO)<sub>9</sub>( $\mu_4$ -C<sub>6</sub>H<sub>8</sub>)( $\eta^6$ -C<sub>6</sub>H<sub>6</sub>)] [24], which consists of a Ru<sub>4</sub> butterfly bridged by a cyclohexyne

ligand with a benzene ring coordinated to one of the wing-tip atoms, hence suggesting that the two structures are closely related. The mass spectrum of **3** exhibits a strong molecular ion peak at 864 (calc. = 863) amu together with peaks corresponding to the sequential loss of nine CO groups. This spectrum indicates that the cluster contains only one diphenylbutadiene ligand and has the general formula, [Ru<sub>4</sub>(CO)<sub>9</sub>(Ph(CH)<sub>4</sub>Ph)], indicating that both the alkyne and arene functionalities coordinate to the cluster from the same ligand rather than from two separate ones. The bonding of the diphenylbutadiene ligand was further substantiated by <sup>1</sup>H NMR spectroscopy. The uncoordinated phenyl ring gives rise to a complicated series of signals between  $\delta$  7.40 and 7.05 ppm. Signals at  $\delta$  6.43, 5.92, 5.82, 5.63 and 4.00 ppm are thought to arise from the five inequivalent protons of the  $\eta^6$  bound phenyl ring. The resonances at  $\delta$  5.92, 5.82 and 5.63 ppm lie within the expected chemical shift range for protons bound to terminally coordinated arene ligands (cf.  $\delta$  5.67 ppm in [Ru<sub>4</sub>(CO)<sub>9</sub>( $\mu_4$ -C<sub>6</sub>H<sub>8</sub>)( $\eta^6$ -C<sub>6</sub>H<sub>6</sub>)] [24]), while those at  $\delta$  6.43 and 4.00 ppm appear at slightly higher and lower frequencies, respectively, than expected for  $\eta^6$ -bound ligands. This suggests that the coordinated phenyl ring may interact with the wingtip ruthenium atom in an asymmetrical fashion such that one proton is closer to a metal atom than the other. Finally, the four multiplet resonances at  $\delta$  5.01, 3.44, 2.56 and 2.30 ppm may be assigned to the four aliphatic protons of the ligand.

These inferences were confirmed by a single crystal X-ray diffraction analysis on a crystal of **3** grown from a dichloromethane–pentane solution at –25°C. The molecular structure of compound **3** is displayed in Fig. 3 with key structural parameters listed in Table 3. Compound **3** crystallises with two independent, *pseudo*-centrosymmetrically related, molecules (**3** and **3'**) in the asymmetric unit, which show no significant differences within the reported esd values.

The Ru<sub>4</sub> skeleton of [Ru<sub>4</sub>(CO)<sub>9</sub>( $\mu_4$ -PhC<sub>2</sub>(CH<sub>2</sub>)<sub>2</sub>- $\eta^6$ -C<sub>6</sub>H<sub>5</sub>)] **3**, takes the form of a butterfly. In common with other butterfly structures of ruthenium, the hinge of the cluster [Ru(1)–Ru(3)] is significantly longer than the other four edges [2.782(3) vs. mean 2.721(3) Å], and the dihedral angle between the two butterfly wings [Ru(1)Ru(2)Ru(3)–Ru(1)Ru(3)Ru(4)] of 109° is slightly less than is commonly observed (112–118°) in related M<sub>4</sub>C<sub>2</sub> systems [25]. This acuteness is thought to arise from the steric restrictions imposed on the Ru<sub>4</sub> framework by the nature of the coordinated ligand.

The organic ligand in **3** may be considered in two parts: Firstly, there is an alkyne unit [C(16)–C(17)], derived via double C–H bond activation of an unsaturated bond within the diphenylbutadiene C<sub>4</sub> chain, positioned between the two wings of the butterfly. The C–C multiple bond is disposed parallel to the hinge and coordinates to all four metal atoms of the cluster via

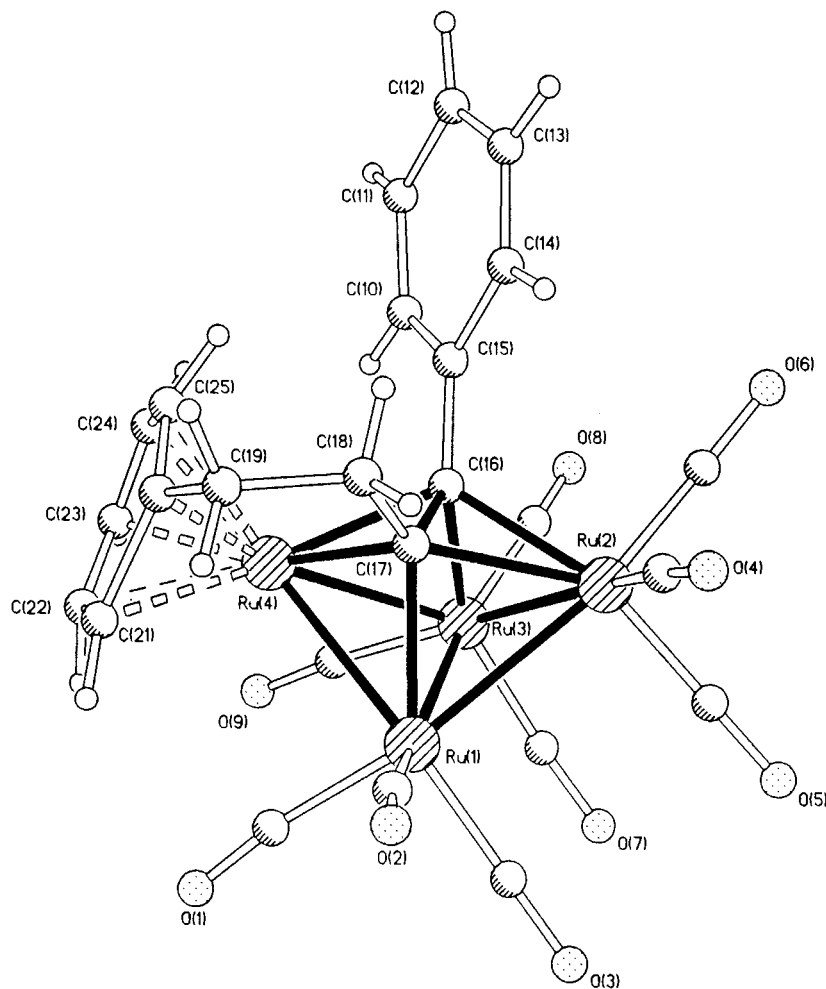


Fig. 3. Molecular structure of **3**, showing the atomic labelling scheme; the C atoms of the CO groups bear the same numbering as the corresponding O atoms.

two  $\sigma$ -interactions with the hinge atoms [Ru(1)–C(17), Ru(3)–C(16)] and two  $\pi$ -interactions with the wing-tip atoms [Ru(2)–C(16), Ru(2)–C(17), Ru(4)–C(16), Ru(4)–C(17)]. This alkyne coordination mode is very similar to that observed in a number of acetylenic, cyclohexyne or cyclooctadieneic butterfly cluster complexes, e.g. [Ru<sub>4</sub>(CO)<sub>12</sub>(C<sub>2</sub>R<sub>2</sub>)] (R = Ph, Me) [14,26], [Ru<sub>4</sub>(CO)<sub>12</sub>( $\mu_4$ -L)] [L = C<sub>6</sub>H<sub>8</sub> [24], C<sub>8</sub>H<sub>10</sub>, and C<sub>8</sub>H<sub>12</sub> [27]] and [Ru<sub>4</sub>(CO)<sub>11</sub>( $\mu_4$ -C<sub>8</sub>H<sub>10</sub>)] [27]. Secondly, the phenyl ring on C(19) interacts with a wing-tip atom of the butterfly cluster [Ru(4)] in a terminal  $\eta^6$ -fashion. The alkyne unit [C(16)–C(17)] and phenyl ring [C(20)–C(25)] are linked through the remaining C<sub>2</sub> section of the ligand [(C(18)–C(19))]. In the original diphenylbutadiene ligand these carbons were sp<sup>2</sup> hybridised, however bond lengths and angles suggest that they now form a saturated –CH<sub>2</sub>CH<sub>2</sub>– linkage and are hence considered as sp<sup>3</sup> carbons. This observation is in keeping with NMR data and migration of the two H-atoms from the alkyne moiety to reduce the torsional strain in this section of the ligand is easy to envisage.

The alkyne C(16)–C(17) bond is not symmetrically positioned with respect to the hinge but lies slightly closer to the ruthenium atom bearing the  $\eta^6$ -phenyl group [Ru(4)], probably as a result of the strain imposed by the linking CH<sub>2</sub>CH<sub>2</sub> unit. This strain also causes a tilting of the coordinated phenyl ring as evidenced by a slight but gradual increase in Ru–C bond distances as we pass from the *ipso*-carbon [Ru(4)–C(20) 2.07(3) Å], through the *ortho*-[Ru(4)–C(21) 2.15(3), Ru(4)–C(25) 2.12(3) Å] and *meta*-[Ru(4)–C(22) 2.19(3), Ru(4)–C(24) 2.19(3) Å] carbons to the *para*-carbon [Ru(4)–C(23) 2.23(3) Å]. Nine carbonyl ligands complete the structural description of **3**; these are all terminal and are distributed evenly over the three ruthenium atoms not involved in bonding to the phenyl ring.

According to the EAN formalism, cluster **3** (butterfly framework; 5 M–M bonds) should be associated with 62 electrons if it is to be considered electron precise. However, if the alkyne ligand is considered as a 4-electron donor then the electron count appears to be 2 electrons short suggesting that a description in terms of

Table 3  
Bond lengths (Å) and angles (°) for the two independent molecules of **3** (**3** and **3'**)

<b>3</b>		<b>3'</b>	
Ru(1)–Ru(2)	2.736(3)	Ru(5)–Ru(6)	2.787(3)
Ru(1)–Ru(3)	2.782(3)	Ru(5)–Ru(7)	2.671(3)
Ru(1)–Ru(4)	2.691(3)	Ru(5)–Ru(8)	2.726(3)
Ru(2)–Ru(3)	2.739(4)	Ru(6)–Ru(7)	2.746(3)
Ru(3)–Ru(4)	2.718(3)	Ru(6)–Ru(8)	2.729(3)
Ru(1)–C(17)	2.18(3)	Ru(5)–C(117)	2.17(3)
Ru(2)–C(16)	2.20(2)	Ru(6)–C(116)	2.15(3)
Ru(2)–C(17)	2.25(2)	Ru(7)–C(116)	2.20(3)
Ru(3)–C(16)	2.13(3)	Ru(7)–C(117)	2.07(3)
Ru(4)–C(16)	2.16(3)	Ru(8)–C(116)	2.18(2)
Ru(4)–C(17)	2.09(2)	Ru(8)–C(117)	2.26(3)
Ru(4)–C(20)	2.07(3)	Ru(7)–C(120)	2.11(3)
Ru(4)–C(21)	2.15(4)	Ru(7)–C(121)	2.18(3)
Ru(4)–C(22)	2.19(3)	Ru(7)–C(122)	2.26(2)
Ru(4)–C(23)	2.23(3)	Ru(7)–C(123)	2.23(3)
Ru(4)–C(24)	2.19(3)	Ru(7)–C(124)	2.17(3)
Ru(4)–C(25)	2.12(3)	Ru(7)–C(125)	2.14(3)
mean Ru–C <sub>(CO)</sub>	1.87(3)	mean Ru–C <sub>(CO)</sub>	1.90(3)
mean C–O	1.18(3)	mean C–O	1.15(3)
mean C–C <sub>(free phenyl)</sub>	1.41(4)	mean C–C <sub>(free phenyl)</sub>	1.37(4)
mean C–C <sub>(η<sup>6</sup>-phenyl)</sub>	1.38(4)	mean C–C <sub>(η<sup>6</sup>-phenyl)</sub>	1.40(4)
C(15)–C(16)	1.43(4)	C(115)–C(116)	1.58(4)
C(16)–C(17)	1.55(3)	C(116)–C(117)	1.49(4)
C(17)–C(18)	1.48(4)	C(117)–C(118)	1.50(4)
C(18)–C(19)	1.47(4)	C(118)–C(119)	1.64(3)
C(19)–C(20)	1.47(4)	C(119)–C(120)	1.52(4)
C(15)–C(16)–C(17)	124(3)	C(115)–C(116)–C(117)	125(2)
C(16)–C(17)–C(18)	127(2)	C(116)–C(117)–C(118)	127(2)
C(17)–C(18)–C(19)	117(3)	C(117)–C(118)–C(119)	112(2)
C(18)–C(19)–C(20)	111(3)	C(118)–C(119)–C(120)	108(2)
Ru(1)Ru(2)Ru(3)– Ru(1)Ru(3)Ru(4)	109	Ru(5)Ru(6)Ru(7)– Ru(5)Ru(6)Ru(8)	110.1

two centre-two electron bonds is inadequate for a cluster of this type. It is therefore better to rationalise the structure and bonding in **3** using PSEPT which, as for **2**, considers the skeletal framework of **3** in terms of a  $M_xC_y$  polyhedron; the two alkyne carbon atoms occupying the vacant sites of the *arachno*  $M_4$  butterfly structure, hence leading to a *pseudo closo*-octahedral  $M_4C_2$  description. If treated as such, the electron count is in accordance with Wade's rules as 6 skeletal atoms are held together by 7 ( $n + 1$ ) skeletal electron pairs.

Thermal activation reactions between  $[Ru_3(CO)_{12}]$  and alkyne ligands have been studied in some detail and shown to a yield a range of cluster derivatives [19]. For example, the reaction with diphenylacetylene results in the formation of  $[Ru_3(CO)_{10}(C_2Ph_2)]$  and  $[Ru_4(CO)_{12}(C_2Ph_2)]$ . If chemical rather than thermal activation methods are employed, however, the reactions often result in different products. The dropwise addition of four molar equivalents of the oxidative decarbonylation reagent trimethylamine N-oxide ( $Me_3NO$ ) to a dichloromethane solution of **1** and diphenylacetylene leads to the formation of two main products which may be readily separated by thin layer

chromatography (tlc) using hexane–dichloromethane (7:3, v/v) as the eluent. The major product has been characterised by spectroscopy as the known bimetallic complex,  $[Ru_2(CO)_6(\mu\text{-}(C_2Ph_2)_2CO)]$  **4** [28], in which two diphenylacetylene units are linked through a carbonyl group and each of the alkyne moieties coordinates to the ruthenium dimer via one  $\pi$  and one  $\sigma$ -interaction. Spectroscopic details for **4** are given in Table 1 and the gross features of the molecule are shown in Fig. 4. The other product has been characterised as the new cluster,  $[Ru_4(CO)_{11}(\mu_4\text{-PhCCPh})_2]$  **5**.

The mass spectrum of **5** exhibits a molecular ion peak at 1071 (calc. = 1069) amu together with peaks corresponding to the sequential loss of eleven carbonyl groups. The  $^1H$  NMR spectrum of **5** displays two multiplet resonances with relative integrals in the ratio 2:3 at  $\delta$  6.72 and 6.93 ppm. These may readily be assigned to the protons of the four phenyl rings, and indicate the equivalence on the NMR timescale of the two alkyne ligands in the complex.

The molecular structure of **5** was confirmed by X-ray crystallography using single crystals grown from a toluene solution at  $-25^\circ C$ , and is shown in Fig. 5 with relevant bond lengths and angles listed in Table 4. The four ruthenium atoms of the cluster adopt a tetrahedrally distorted square arrangement with Ru(1), Ru(2), Ru(3) and Ru(4) being  $-0.3190$ ,  $-0.3203$ ,  $0.3198$ , and  $0.3194$  Å, respectively, out of the mean least-squares plane that passes through them. Two edges, on opposite sides of the square, are longer than the other two [Ru(1)–Ru(4) 2.8370(7), Ru(2)–Ru(3) 2.8305(7) vs. Ru(1)–Ru(3) 2.7718(8), Ru(2)–Ru(4) 2.7682(9) Å] and the shortest edge, Ru(2)–Ru(4), is spanned by a near-symmetrically bridging carbonyl group [Ru(2)–C(23) 2.051(5), Ru(4)–C(23) 2.083(5) Å]. The diphenylacetylene ligands diagonally straddle opposite faces of the square cluster such that the C–C alkyne bonds are perpendicularly disposed to one another. Each ligand interacts with the cluster in a  $\mu_4\text{-}\sigma:\sigma:\pi:\pi$  manner; two  $\sigma$ -bonds are formed between the alkyne carbons and two ruthenium atoms in opposite corners of the square, while two  $\pi$ -bonds are

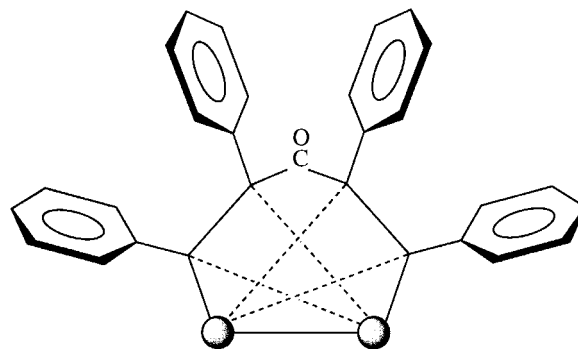


Fig. 4. Representation of compound **4** showing carbonyl insertion between two alkyne ligands.

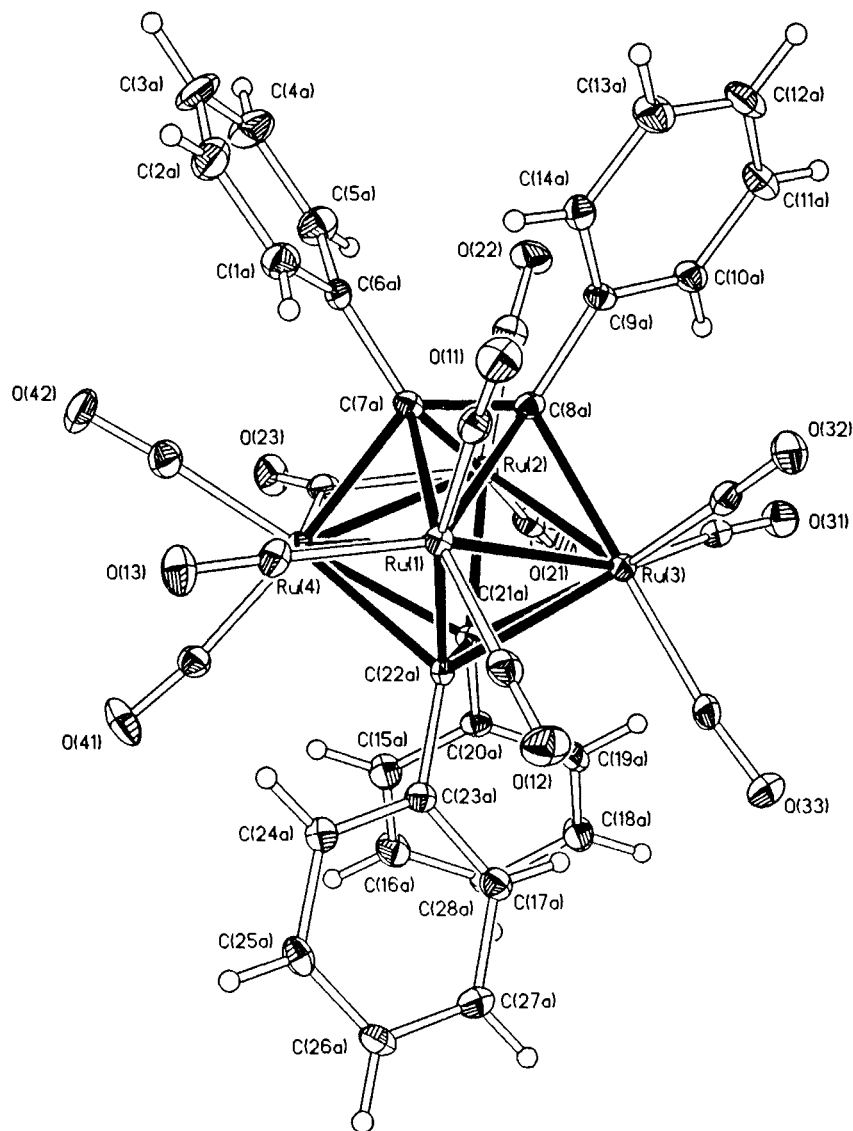


Fig. 5. Molecular structure of **5**, showing the atomic labelling scheme; the C atoms of the CO groups bear the same numbering as the corresponding O atoms.

Table 4  
Bond lengths (Å) and angles (°) for **5**

Ru(1)–Ru(3)	2.7718(8)	C(7a)–C(8a)	1.404(6)
Ru(1)–Ru(4)	2.8370(7)	C(21a)–C(22a)	1.406(6)
Ru(2)–Ru(3)	2.8305(7)	C(6a)–C(7a)	1.516(6)
Ru(2)–Ru(4)	2.7682(9)	C(8a)–C(9a)	1.510(6)
Ru(1)–C(7a)	2.303(4)	C(20a)–C(21a)	1.508(6)
Ru(1)–C(8a)	2.476(5)	C(22a)–C(23a)	1.501(6)
Ru(1)–C(22a)	2.182(4)	mean C–C <sub>(phenyl)</sub>	1.382(7)
Ru(2)–C(7a)	2.366(4)	mean Ru–C <sub>(termCO)</sub>	1.907(5)
Ru(2)–C(8a)	2.285(4)	mean C–O <sub>(term CO)</sub>	1.135(6)
Ru(2)–C(21a)	2.185(4)	Ru(2)–C(23)	2.051(5)
Ru(3)–C(8a)	2.181(4)	Ru(4)–C(23)	2.083(5)
Ru(3)–C(21a)	2.311(4)	C(23)–O(23)	1.154(5)
Ru(3)–C(22a)	2.434(4)		
Ru(4)–C(7a)	2.197(4)	Ru(1) ⋯ Ru(2)	3.854
Ru(4)–C(21a)	2.371(4)	Ru(3) ⋯ Ru(4)	3.862
Ru(4)–C(22a)	2.334(4)		

formed between the same two carbon atoms and the other two ruthenium atoms. Therefore each ruthenium atom of the cluster interacts with one alkyne ligand via a  $\sigma$ -bond [mean Ru–C<sub>( $\sigma$ )</sub> 2.186(4) Å] and with the other via a  $\pi$ -bond [mean Ru–C<sub>( $\pi$ )</sub> 2.360(4) Å]. A view of the alkyne-cluster bonding interactions is shown in Fig. 6. The coordination sphere of the cluster is completed by the presence of ten terminal and essentially linear carbonyl ligands which are arranged with three on Ru(1) and Ru(2) and two on Ru(3) and Ru(4).

As before, the cluster framework in **5** may be described in terms of a  $M_xC_y$  polyhedron. In this case the cluster has a  $Ru_4C_4$  core in which the ruthenium and carbon atoms sit at the vertices of a triangulated dodecahedron. This dodecahedron may be envisaged as a pair of interpenetrating distorted tetrahedra; an elongated  $C_4$

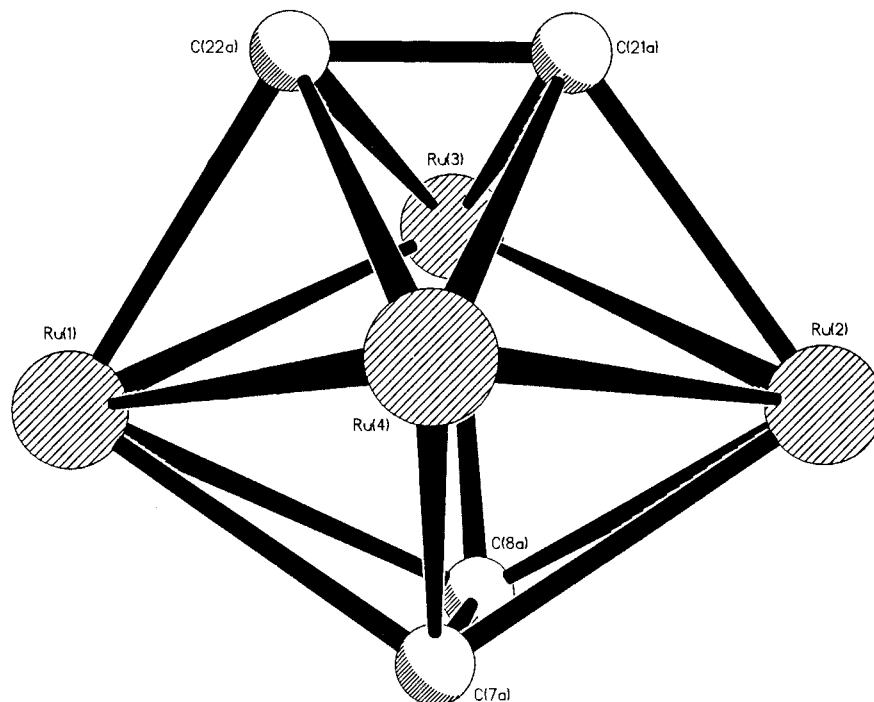


Fig. 6. The bonding interactions between the cluster and the two diphenylacetylene ligands in **5**; a view of the  $\text{Ru}_4\text{C}_4$  dodecahedral core.

core and a flattened  $\text{Ru}_4$  core. This structure is very similar to those already found for  $[\text{Fe}_4(\text{CO})_{11}(\text{EtCCH})_2]$  [18] and  $[\text{Ru}_4(\text{CO})_{11}(\text{MeC}_2\text{Ph})_2]$  [29] all of which have 8 vertices held together by 9 ( $n + 1$ ) skeletal electron pairs.

### 3. Concluding remarks

The idea of considering organometallic clusters as *closo*-, *nido*- and *arachno*-forms and, in the case of  $\text{Ru}(\text{CO})_3$  fragments, allied to the structures of the carboranes is clearly very attractive. It certainly leads to a consideration of a wide variety of complexes which could not have been visualised from the simpler valence bond approach in which the organo fragment is considered primarily as an addendum to the 'preformed' cluster. A feature mainly associated with the carboranes, however, is the added availability of capped polyhedral forms. Although this aspect has not been covered in this paper it is an additional and important feature of organometallic cluster chemistry which should be developed in a future report.

### 4. Experimental

All reactions were carried out under nitrogen gas using dry, freshly distilled solvents. Infrared spectra were recorded on a Perkin Elmer 1600 Series FTIR Spectrometer using NaCl cells (pathlength 0.5 mm).

Fast atom bombardment (FAB) mass spectra were obtained using a Kratos MS50TC spectrometer.  $^1\text{H}$  NMR spectra were recorded on Bruker WH 200 and WH 400 instruments in  $\text{CDCl}_3$  referenced to internal TMS. Products were separated by thin layer chromatography (TLC) on plates supplied by Merck coated with a 0.25 mm layer of Kieselgel 60  $\text{F}_{254}$  or by column chromatography through silica gel Kieselgel 60, particle size 0.040–0.063 mm, mesh size 230–400ASTM, also supplied by Merck. The cluster  $[\text{Ru}_3(\text{CO})_{12}]$  **1** was prepared by the literature procedure [30]. Trimethylamine N-oxide ( $\text{Me}_3\text{NO}$ ), purchased from Aldrich Chemicals as the dihydrate, was dried by a Dean and Stark distillation in benzene and sublimation immediately prior to reaction. Diphenylacetylene and diphenylbutadiene were also purchased from Aldrich Chemicals and used without further purification.

#### 4.1. Reaction of $[\text{Ru}_3(\text{CO})_{12}]$ **1** with 1,4-diphenylbutadiene:

The cluster  $[\text{Ru}_3(\text{CO})_{12}]$  **1** (500 mg, 0.782 mmol) and  $\text{PhC}_4\text{Ph}$  (484 mg, 2.346 mmol) were suspended in octane (50 ml) and heated to reflux for 5 h. The solvent was removed in vacuo and three main products isolated from the reaction mixture by column chromatography using  $\text{CH}_2\text{Cl}_2$ /hexane (1:4, v/v) as eluent. These have been characterised as  $[\text{Ru}_3(\text{CO})_8(\mu_3\text{-CPh}(\text{CH})_2\text{CPh})]$  (yellow, 18%) **2** and  $[\text{Ru}_4(\text{CO})_9(\mu_4\text{-CPhCCH}_2\text{CH}_2\text{Ph})]$  (purple, 21%) **3**. Orange crystals of **2** were obtained from a toluene solution at  $-25^\circ\text{C}$ . Purple crystals of **3**



were obtained from a  $\text{CH}_2\text{Cl}_2$ /pentane solution at  $-25^\circ\text{C}$ .

#### 4.2. Reaction of $[\text{Ru}_3(\text{CO})_{12}]$ with diphenylacetylene:

A dichloromethane (100 ml) solution of  $[\text{Ru}_3(\text{CO})_{12}]$  **1** (100 mg, 0.156 mmol) and  $\text{PhC}_2\text{Ph}$  (54 mg, 0.303 mmol) was treated with  $\text{Me}_3\text{NO}$  (45 mg, 0.600 mmol) in dichloromethane (30 ml) at  $-78^\circ\text{C}$ . The solution was warmed to room temperature over 30 min and the solvent removed in vacuo. Two major products have been isolated by TLC using  $\text{CH}_2\text{Cl}_2$ /hexane (3:7, v/v) as eluent, and fully characterised by spectroscopy as the known cluster  $[\text{Ru}_2(\text{CO})_6(\mu\text{-}\{\text{C}_2\text{Ph}_2\}_2\text{CO})]$  (yellow, 24%) **4**, and the new cluster  $[\text{Ru}_4(\text{CO})_{11}(\mu_4\text{-PhCCPh})_2]$  (orange 18%) **5**. Dark orange crystals of **5** were obtained from a toluene solution at  $-25^\circ\text{C}$ .

#### 4.3. Crystal structure determination for compounds **2**, **3** and **5**

##### 4.3.1. Crystal data:

Complex **2** crystallises with half a molecule in the asymmetric unit [there is a diad through  $\text{Ru}(2)$ ];  $\text{C}_{24}\text{H}_{12}\text{O}_8\text{Ru}_3$ ,  $M = 731.55$ , Monoclinic, space group  $\text{C}2/c$ ,  $a = 12.110(2)$ ,  $b = 13.163(3)$ ,  $c = 14.670(3)$  Å,  $\beta = 95.61(3)^\circ$ ,  $U = 2327.3(8)$  Å<sup>3</sup>,  $\lambda = 0.71069$  Å,  $Z = 4$ ,  $D_c = 2.088$  Mg/m<sup>3</sup>, yellow crystal  $0.20 \times 0.20 \times 0.20$  mm,  $\mu(\text{Mo-K}\alpha) = 1.970$  mm<sup>-1</sup>,  $F(000) = 1408$ . **3**: Complex **3** crystallises with two independent, *pseudo*-centrosymmetrically related, molecules in the asymmetric unit;  $\text{C}_{25}\text{H}_{14}\text{O}_9\text{Ru}_4$ ,  $M = 862.64$ , Orthorhombic, space group  $\text{Pca}2(1)$ ,  $a = 18.715(6)$ ,  $b = 16.404(6)$ ,  $c = 16.335(7)$  Å,  $U = 5015(3)$  Å<sup>3</sup>,  $\lambda = 0.71069$  Å,  $Z = 8$ ,  $D_c = 2.285$  Mg/m<sup>3</sup>, dark needle  $0.20 \times 0.10 \times 0.10$  mm,  $\mu(\text{Mo-K}\alpha) = 2.416$  mm<sup>-1</sup>,  $F(000) = 3296$ . **5**: Complex **5** crystallises with a molecule of toluene solvent in the asymmetric unit;  $\text{C}_{46}\text{H}_{28}\text{O}_{11}\text{Ru}_4$ ,  $M = 1160.96$ , Monoclinic, space group  $\text{P}2(1)/n$ ,  $a = 13.428(3)$ ,  $b = 15.600(3)$ ,  $c = 20.447(4)$  Å,  $\beta = 106.09(3)^\circ$ ,  $U = 4115(2)$  Å<sup>3</sup>,  $\lambda = 0.71069$  Å,  $Z = 4$ ,  $D_c = 1.874$  Mg/m<sup>3</sup>, orange crystal,  $0.30 \times 0.15 \times 0.13$  mm,  $\mu(\text{Mo-K}\alpha) = 1.503$  mm<sup>-1</sup>,  $F(000) = 2272$ .

##### 4.3.2. Data collection and processing:

All X-ray measurements were made on a RIGAKU AFC7R diffractometer equipped with an Oxford Cryosystems low-temperature device, graphite-monochromated  $\text{Mo-K}\alpha$  X-ray: **2**;  $T = 293(2)$  K,  $\omega$ - $2\theta$  scans, 2675 independent reflections collected ( $2\theta_{\text{max}} 45^\circ$ ,  $h$  0 to 15,  $k$  0 to 17,  $l$ -19 to 18), semi-empirical absorption correction applied giving 2234 unique reflections with  $I > 2\sigma(I)$  for use in all calculations. **3**;  $T = 150(2)$  K,  $\omega$ - $2\theta$  scans, 3867 independent reflections collected ( $2\theta_{\text{max}} 50^\circ$ ,  $h$ -22 to 0,  $k$ -19 to 19,  $l$  0 to

17), semi-empirical absorption correction applied, giving 2456 reflections with  $I > 2\sigma(I)$  for use in all calculations. **5**,  $T = 150(2)$  K,  $\omega$ - $2\theta$  scans, 7243 independent reflections collected ( $2\theta_{\text{max}} 50^\circ$ ,  $h$  0 to 15,  $k$  0 to 18,  $l$ -24 to 23), semi-empirical absorption correction applied, giving 5774 reflections with  $I > 2\sigma(I)$  for use in all calculations.

##### 4.3.3. Structure solution and refinement:

The ruthenium atoms were located by automatic direct methods [31], and subsequent iterative cycles of least-squares refinement and Fourier difference synthesis located all non-H atoms [32]. In **2** and **5** all non-H atoms were then refined (by least-squares on  $F^2$ ) with anisotropic thermal parameters, whereas in **3** (because the two independent molecules in the asymmetric unit are related by a *pseudo*-centre of symmetry) only the Ru atoms were refined anisotropically, with the remaining non-H atoms allowed isotropic thermal motion. H-atoms were included in the models in idealised positions and allowed to ride on the C-atoms with isotropic thermal parameters fixed at  $0.08$  Å<sup>3</sup> and C–H distances at  $0.96$  Å. Strenuous efforts were made to refine **3** in a centrosymmetric space group, however, no solution was obtained in space group  $\text{Pbcm}$ , and a trial solution in  $\text{Pbca}$  refined unsatisfactorily to  $R1 = 0.1789$ .

In **2** at final convergence  $R1 = 0.0274$  [using 2234 intensity data with  $I > 2\sigma(I)$ ] and  $wR2 = 0.1710$  [all data, calc.  $w = 1/[\sigma^2(F_o^2) + (0.0268P)^2 + 3.79P]$  where  $P = (F_o^2 + 2F_c^2)/3$ ],  $S = 1.043$  for 159 refined parameters. The largest peak in the difference Fourier map was  $0.67$  eÅ<sup>-3</sup>. In **3** at final convergence  $R1 = 0.0625$  [using 2456 intensity data with  $I > 2\sigma(I)$ ] and  $wR2 = 0.1124$  [all data, calc.  $w = 1/[\sigma^2(F_o^2) + (0.0053P)^2 + 0.18P]$  where  $P = (F_o^2 + 2F_c^2)/3$ ],  $S = 1.012$  for 345 refined parameters. The largest peak in the difference Fourier map was  $1.14$  eÅ<sup>-3</sup>. In **5** at final convergence  $R1 = 0.0342$  [using 5774 intensity data with  $I > 2\sigma(I)$ ] and  $wR2 = 0.0734$  [all data, calc.  $w = 1/[\sigma^2(F_o^2) + (0.0206P)^2 + 2.18P]$  where  $P = (F_o^2 + 2F_c^2)/3$ ],  $S = 1.021$  for 551 refined parameters. The largest peak in the difference Fourier map was  $0.45$  eÅ<sup>-3</sup>.

Additional material available from the Cambridge Crystallographic Data Centre comprises H-atom coordinates, thermal parameters and the remaining bond lengths and angles.

#### Acknowledgements

We would like to thank the EPSRC (R.H.H.P.), the Newton Trust (R.H.H.P.) ICI (Wilton) (C.M.M.) and The University of Cambridge for Financial support.

## References

- [1] E.L. Muetterties, T.N. Rhodin, E. Band, C.F. Bruker, W.R. Pretzer, *Chem. Rev.* 79 (1979) 91.
- [2] D.M.P. Mingos, *Nature Phys. Sci. (London)* 236 (1972) 99.
- [3] K. Wade, *Adv. Inorg. Chem. Radiochem.* 18 (1976) 1.
- [4] S.M. Owen, *Polyhedron* 7 (1988) 253, and references cited therein.
- [5] K. Wade, *Transition Metal Clusters*, in: B.F.G. Johnson (Ed.), Wiley-Interscience, Chichester, 1980, Chap. 3 and references cited therein.
- [6] F.A. Cotton, J.D. Jamerson, B.R. Stutts, *J. Am. Chem. Soc.* 98 (1976) 1774.
- [7] L.V. Rybin, E.A. Petrovskaya, Y.T. Struchkov, A.S. Batsanov, M.I. Rybinskaya, *J. Organomet. Chem.* 226 (1982) 63.
- [8] A.C. Villa, L. Coghi, A.G. Manfredotti, C. Guastini, *Acta Crystallogr. Sect. B* 30 (1974) 2101.
- [9] J.F. Blount, L.F. Dahl, C. Hoogzand, W. Hubel, *J. Am. Chem. Soc.* 88 (1966) 292.
- [10] C.G. Pierpoint, *Inorg. Chem.* 16 (1977) 636.
- [11] J.S. Bradley, S. Harris, J.M. Newsam, E.W. Hill, S. Leta, M.A. Modrick, *Organometallics* 6 (1987) 2060.
- [12] A.A. Hock, O.S. Mills, *Acta Crystallogr.* 14 (1961) 139.
- [13] S. Aime, A. Tiripicchio, M. Tiripicchio Camellini, A.J. Deeming, *Inorg. Chem.* 20 (1981) 2027.
- [14] B.F.G. Johnson, J. Lewis, B.E. Reichert, K.T. Schorpp, G.M. Sheldrick, *J. Chem. Soc., Dalton Trans.*, 1977, 1417.
- [15] E. Rosenberg, S. Aime, L. Milone, E. Sappa, A. Tiripicchio, A.M. Manotti Lanfredi, *J. Chem. Soc., Dalton Trans.*, 1981, 2023.
- [16] M.K. Alami, F. Dahan, R. Mathieu, *Organometallics* 4 (1985) 2112.
- [17] M.P. Gomez-Sal, B.F.G. Johnson, R.A. Kamarudin, J. Lewis, P.R. Raithby, *J. Chem. Soc., Chem. Comm.*, 1985, 1622.
- [18] E. Sappa, A. Tiripicchio, M. Tiripicchio Camellini, *J. Chem. Soc., Dalton Trans.*, 1978, 419.
- [19] P.R. Raithby, M.J. Rosales, *Adv. Inorg. Chem. Radiochem.* 2 (1985) 169.
- [20] R.P. Dodge, V. Schomaker, *J. Organomet. Chem.* 3 (1965) 274.
- [21] D. Nuel, F. Dahan, R. Mathieu, *J. Am. Chem. Soc.* 107 (1985) 1658.
- [22] B. Heim, J.C. Daran, Y. Jeannin, B. Eber, G. Huttner, W. Imhof, *J. Organomet. Chem.* 441 (1992) 81.
- [23] D. Lentz, H.M. Schulz, M. Reuter, *Organometallics* 11 (1992) 2916.
- [24] D. Braga, F. Grepioni, J.J. Byrne, C.M. Martin, B.F.G. Johnson, A.J. Blake, *J. Chem. Soc., Dalton Trans.*, 1995, 1555.
- [25] S. Sapa, A. Tiripicchio, A.J. Carty, G.E. Toogood, *Prog. Inorg. Chem.* 35 (1987) 437.
- [26] P.F. Jackson, B.F.G. Johnson, J. Lewis, P.R. Raithby, G.J. Will, M. McPartlin, W.J.H. Nelson, *J. Chem. Soc., Chem. Comm.*, 1980, 1190.
- [27] A.J. Carty, A.J.P. Domingos, B.F.G. Johnson, J. Lewis, *J. Chem. Soc., Dalton Trans.*, 1973, 2056.
- [28] A.J. Blake, P.J. Dyson, S.L. Ingham, B.F.G. Johnson, C.M. Martin, *Organometallics* 14 (1995) 862.
- [29] S. Aime, G. Nicola, D. Osella, A.M.M. Lanfredi, A. Tiripicchio, *Inorg. Chim. Acta* 85 (1984) 161.
- [30] C.R. Eady, P.F. Jackson, B.F.G. Johnson, J. Lewis, M.C. Malatesta, M. McPartlin, W.J.H. Nelson, *J. Chem. Soc., Dalton Trans.*, 1980, 383.
- [31] G.M. Sheldrick, SHELXS 86, Program for Crystal Structure Solution, *Acta Crystallogr. Sect. A* 46 (1990) 467.
- [32] G.M. Sheldrick, SHELXL 93, Program for Crystal Structure Refinement, Univ. of Gottingen, 1993.